

and phosphoramidates. In a few cases, however, the value of  $\beta_{\text{nuc}}$  is near zero or even negative. For the phosphorylation of substituted pyridines by 2,4-dinitrophenyl phosphate,  $\beta_{\text{nuc}}$  is approximately zero;<sup>3b</sup> for the phosphorylation of quinuclidines by *N*-phospho-4-morpholinopyridine,  $\beta_{\text{nuc}} = -0.01$ ;<sup>16</sup> for the phosphorylation of quinuclidines by 2,4-dinitrophenyl phosphate,  $\beta_{\text{nuc}} = -0.10$ ;<sup>16</sup> for the phosphorylation of primary amines by *p*-nitrophenyl phosphate,  $\beta_{\text{nuc}} = -0.05$ .<sup>16</sup> Jencks and co-workers explain the negative values of  $\beta_{\text{nuc}}$  on the basis that nucleophiles are solvated in aqueous solution and their reactions with phosphate compounds require their desolvation or partial desolvation.<sup>16</sup> The effect of increasing  $\text{p}K_{\text{a}}$  on the desolvation should be to decrease the rate, the opposite of its effect on nucleophilic reactivity, because solvent should be increasingly strongly held by nucleophiles of increasing basicity. Therefore, the second-order rate constants for the reactions as nucleophiles can be sensitive to desolvation in cases in which desolvation limits the rate at which the nucleophile undergoes phosphorylation and the negative values of  $\beta_{\text{nuc}}$  represent the effects of  $\text{p}K_{\text{a}}$  on the desolvation of the nucleophiles. In the case of MTP,  $\beta_{\text{nuc}}$  cannot be measured because of the absence of a second-order term for the nucleophile in the rate law; that is, there is no nucleophilic participation in the transition state.

In concluding that discrete monomeric metaphosphate is not an intermediate in solvolysis reactions in aqueous solutions, Herschlag and Jencks have estimated that discrete metaphosphate could be generated on a reaction trajectory between nitrogen and oxygen bases if the  $\text{p}K_{\text{nuc}} = -20$  or the  $\text{p}K_{\text{ig}} = -13$ . These estimates do not refer to the transfer of  $\text{PO}_3^-$  between oxygen and sulfur, as in the hydrolysis of MTP. The P-S bond differs from the P-O bond in that it does not participate in resonance delocalization and  $\pi$ -bonding.<sup>14</sup> This difference is attributed by Reed and Schleyer to the relative absence of  $\text{p}_\pi\text{-}\sigma^*$  negative hyperconjugation in the P-S bond compared with the P-O bond.<sup>17</sup> The P-S bond is also weaker than the P-O bond by about 30 kcal mol<sup>-1</sup>.<sup>18</sup> These

bonding differences apparently allow the P-S bond in MTP to undergo cleavage to  $\text{PO}_3^-$  without nucleophilic participation, despite the fact that the  $\text{p}K_{\text{a}}$  of the leaving group,  $\text{HPSO}_3^{2-}$ , is 5.4.

The mechanism of eq 4 is the preassociation mechanism advanced by Jencks as a means by which monomeric metaphosphate might be an intermediate in phosphoryl group transfer reactions that proceed with nucleophilic participation in the transition state.<sup>19</sup> Structure reactivity correlations exclude this mechanism for phosphoryl group transfer between nitrogen bases and between nitrogen and oxygen bases in water.<sup>5c,d</sup> The preassociation stepwise mechanism remains possible for phosphoryl group transfer reactions in aprotic solvents or *t*-butyl alcohol, which proceed with racemization of chiral phosphate.<sup>5c,d</sup> Positional isotope exchange in  $[\beta\text{-}^{18}\text{O}_4]\text{ADP}$  or  $[\alpha,\beta\text{-}^{18}\text{O}]\text{ADP}$  reisolated from solvolysis reactions in acetonitrile can also be explained by the preassociation stepwise mechanism, although the transient participation of acetonitrile to stabilize metaphosphate cannot be excluded.<sup>20</sup> The hydrolysis of MTP seems to follow the preassociation stepwise mechanism in water, in which monomeric metaphosphate appears to be the transient intermediate that is generated in the preassociation complex.

**Acknowledgment.** This research was supported by Grant No. GM30480 from the National Institute of General Medical Sciences. This study made use of the National Magnetic Resonance Facility at Madison, which is supported in part by NIH Grant RR02301 from the Biomedical Research Technology Program, Division of Research Resources. Equipment in the facility was purchased with funds from the University of Wisconsin, the NSF Biological Instrumentation Program (Grant PCM-845048), the NIH Biomedical Research Technology Program (Grant RR20301), the NIH Shared Instrument Program (Grant RR02781), and the U.S. Department of Agriculture.

(16) Jencks, W. P.; Haber, M. T.; Herschlag, D.; Nazaretian, K. L. *J. Am. Chem. Soc.* 1986, 108, 479-483.

(17) Reed, A. E.; Schleyer, P. v. R. *J. Am. Chem. Soc.* 1990, 112, 1434-1445.

(18) (a) Thain, E. M. *J. Chem. Soc.* 1957, 4694-4699. (b) Cottrell, T. L. *The Strengths of Chemical Bonds*, 2nd ed.; Butterworths: London, 1958; pp 270-289.

(19) Jencks, W. P. *Acc. Chem. Res.* 1980, 13, 161-169.

(20) (a) Lowe, G.; Tuck, S. P. *J. Am. Chem. Soc.* 1986, 108, 1300-1301. (b) Cullis, P. M.; Nicholls, P. *J. Chem. Soc., Chem. Commun.* 1987, 783-785.

## General Acid Catalysis of the Reduction of *p*-Benzoquinone by an NADH Analog. Evidence for Concerted Hydride and Hydron Transfer

Charolette A. Coleman, Joseph G. Rose, and Christopher J. Murray\*

Contribution from the Department of Chemistry and Biochemistry, University of Arkansas, Fayetteville, Arkansas 72701. Received July 13, 1992

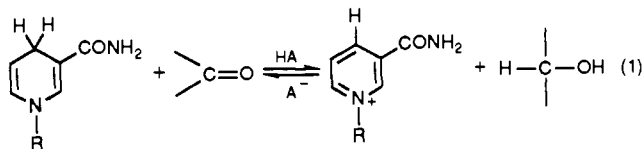
**Abstract:** Rate constants for general acid catalysis of the reduction of *p*-benzoquinone by an NADH analog, [9-<sup>1</sup>H<sub>2</sub>]- and [9-<sup>2</sup>H<sub>2</sub>]-10-methylacridan, were determined in water and deuterium oxide at 25 °C. Catalysis by substituted acetic acids follows a Brønsted correlation with slope  $\alpha = 0.85$ . There is a 60-fold negative deviation for hydronium ion catalysis and a 6-fold positive deviation for catalysis by cacodylic acid. For RCOOH catalysts, solvent isotope effects  $k_{\text{AH}}^{\text{H}}/k_{\text{AD}}^{\text{H}}$  range from 1.2 to 3.0 for [9-<sup>1</sup>L<sub>2</sub>]-10-methylacridans (L = <sup>1</sup>H, <sup>2</sup>H). Substrate deuterium isotope effects  $k_{\text{AL}}^{\text{H}}/k_{\text{AL}}^{\text{D}} = 1.5 \pm 0.1$  in water or deuterium oxide are small and essentially independent of the catalyst  $\text{p}K_{\text{a}}$ . Several reaction mechanisms are discussed, including reactions involving the semiquinone radical and radical anion generated by one-electron transfers. It is concluded that these results are most consistent with a concerted one-step hydride transfer assisted by proton transfer from the catalyst to form 4-hydroxycyclohexa-2,5-dienone that enolizes rapidly to hydroquinone.

### Introduction

We are interested the mechanisms of coupling of hydride transfers from NADH analogs with proton transfers to the carbonyl group (eq 1) for several reasons. First, acids and bases in the active sites of enzymes often play a crucial role in catalyzing

these types of reactions.<sup>1,2</sup> For example, in the case of lactate dehydrogenase, an active site histidine has been implicated as an

(1) Jencks, W. P. *Catalysis in Chemistry and Enzymology*; Dover: New York, 1987; Chapter 3.



electrophilic catalyst to polarize the carbonyl group of pyruvate.<sup>3</sup> Even in cases where the electrophile is a metal ion, active site groups must shuttle a proton from the bulk solvent to the metal-bound alkoxide in order for the product alcohol to be released into solution.<sup>4</sup> In the zinc-dependent horse liver alcohol dehydrogenase this occurs via a proton relay with Ser-48, the ribose 2'-hydroxyl group of NAD<sup>+</sup>, and His-51 that gives rise to an inverse 2-fold solvent isotope effect as well as a 4-fold substrate isotope effect on the transient rate of oxidation of ethanol-*d*<sub>5</sub> in the reverse direction.<sup>5</sup>

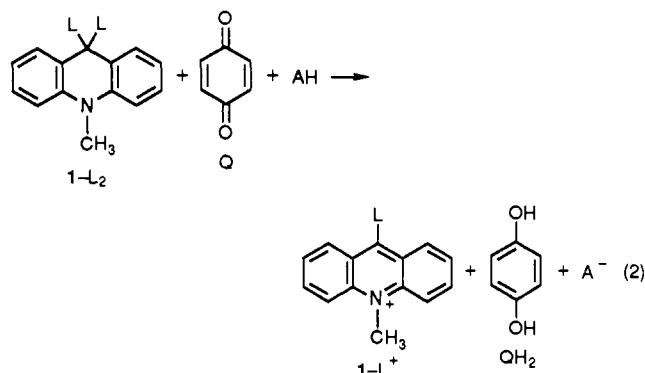
Second, eq 1 describes a type of class e reaction<sup>6</sup> where proton donation to the electrophilic center facilitates nucleophilic attack of the hydride ion equivalent from NADH. It is well established that general acid catalysis of the addition of thiolate<sup>7</sup> and amine<sup>8</sup> nucleophiles to the carbonyl group by class e mechanisms depends upon the lifetime of the addition intermediate formed in the reaction. It is of interest to understand the conditions under which general acid catalysis of similar types of reactions can be observed when no additional intermediate is formed, as in the case of eq 1.

Finally, although extensive model studies of ketone reduction by NADH analogs have shown that metal ions,<sup>9,10</sup> protons,<sup>11</sup> or other general acids<sup>12</sup> can act as electrophilic catalysts, it is not so clear whether the mechanism of Lewis acid-catalyzed ketone reduction can involve intermediate radical ions generated by one-electron transfer from 1,4-dihydropyridine derivatives.<sup>13</sup>

Extensive studies of the *uncatalyzed* transfer of a hydride ion from 1,4-dihydropyridine donors have largely settled the debate as to when a one-step hydride transfer or a sequential electron, proton, and electron transfer pathway will be followed.<sup>13,14</sup> Using isotope effects,<sup>15</sup> as well as other kinetic and thermodynamic data,<sup>16-20</sup> several workers have established that hydride transfers

from 1,4-dihydropyridine donors to acceptors with one-electron reduction potentials  $E^\circ$  greater than 0.4 V (vs NHE at 25 °C) occur through single-electron transfers (SET) mechanisms.<sup>21-24</sup> Most carbonyl compounds have much lower one-electron reduction potentials and are therefore expected to be reduced by one-step hydride transfers. However, for *acid-catalyzed* reactions the interaction of the carbonyl group with Lewis acids may enhance the electron affinity of the substrate so that single electron transfers may provide a favorable reaction pathway for suitably active substrates.<sup>24,25</sup>

We have chosen to re-investigate the reduction of *p*-benzoquinone, Q, by an acid-stable NADH analog, [9-*L*<sub>2</sub>]-10-methylacridan (1-*L*<sub>2</sub>; L = <sup>1</sup>H or <sup>2</sup>H) in a largely aqueous solvent, eq 2. This reaction has been suggested to occur by a one-step



hydride transfer<sup>26-28</sup> as well as SET mechanisms involving the semiquinone radical anion, Q<sup>•-</sup>, and radical, QH<sup>•</sup>.<sup>29</sup> Many of the redox and acid-base properties of these species as well as the radical cation of 10-methylacridan, 1-H<sub>2</sub><sup>•+</sup>, have been determined<sup>30-32</sup> so that it is possible to evaluate their role in the reaction mechanism.

We report here evidence for a one-step hydride transfer mechanism for eq 2 in water. SET mechanisms are excluded. The evidence includes (1) a Brønsted  $\alpha$  value equal to 0.85 for catalysis by substituted acetic acids that does not show a break at  $\text{p}K_a = 4$  as expected for involvement of the semiquinone radical ( $\text{p}K_a^{\text{QH}^\bullet} = 4.1$ )<sup>31</sup> in the mechanism, (2) the absence of any significant buffer curvature up to 0.5 M total buffer that is required for a mechanism

(2) *The Enzymes*, 3rd ed.; Boyer, P. D., Ed.; Academic: New York, 1975; Vol. XI.

(3) Grau, U. M.; Trommer, W. E.; Rossmann, M. G. *J. Mol. Biol.* **1981**, *151*, 289.

(4) Pettersson, G. *CRC Crit. Rev. Biochem.* **1987**, *21*, 349-389. Ehrig, T.; Hurlley, T. D.; Edenberg, H. J.; Bosron, W. F. *Biochemistry* **1991**, *30*, 1062-1068.

(5) Sekhar, V. C.; Plapp, B. V. *Biochemistry* **1990**, *29*, 4289-4295.

(6) Jencks, W. P. *Acc. Chem. Res.* **1976**, *9*, 425-432.

(7) Jencks, W. P. *Acc. Chem. Res.* **1980**, *13*, 161-169.

(8) Cox, M. M.; Jencks, W. P. *J. Am. Chem. Soc.* **1981**, *103*, 572-580.

(9) Ohno, A.; Yamamoto, H.; Oka, S. *J. Am. Chem. Soc.* **1981**, *103*, 2041-2045.

(10) Yasui, S.; Ohno, A. *Bioorg. Chem.* **1986**, *14*, 70-96.

(11) Abeles, R. H.; Hutton, R. F.; Westheimer, F. H. *J. Am. Chem. Soc.* **1957**, *79*, 712-716. Pandit, U. K.; Mas Cabrè, F. R. *J. Chem. Soc., Chem. Commun.* **1971**, 552. Shinkai, S.; Bruice, T. C. *Biochemistry* **1973**, *12*, 1750-1759.

(12) Shinkai, S.; Hamada, H.; Kusano, Y.; Manabe, O. *J. Chem. Soc., Perkin Trans. 2* **1979**, 699-702. Awano, H.; Tagaki, W. *Bull. Chem. Soc. Jpn.* **1986**, *59*, 3117-3123.

(13) Watt, C. I. F. *Adv. Phys. Org. Chem.* **1988**, *24*, 57-112.

(14) Bunting, J. W. *Bioorg. Chem.* **1991**, *19*, 456-491.

(15) Powell, M. F.; Bruice, T. C. *J. Am. Chem. Soc.* **1982**, *104*, 5834-5836. Powell, M. F.; Bruice, T. C. *J. Am. Chem. Soc.* **1983**, *105*, 7139-7149.

(16) Powell, M. F.; Bruice, T. C. *J. Am. Chem. Soc.* **1983**, *105*, 1014-1021.

(17) Roberts, R. M. G.; Ostović, D.; Kreevoy, M. M. *Faraday Discuss. Chem. Soc.* **1982**, *74*, 257-265. Kreevoy, M. M.; Ostović, D.; Lee, I.-S. H.; Binder, D. A.; King, G. W. *J. Am. Chem. Soc.* **1988**, *110*, 524-530. Lee, I.-S. H.; Ostović, D.; Kreevoy, M. M. *J. Am. Chem. Soc.* **1988**, *110*, 3989-3993.

(18) Martens, F. M.; Verhoeven, J. W.; Gase, R. A.; Pandit, U. K.; de Boer, Th. J. *Tetrahedron* **1978**, *34*, 443-446. Verhoeven, J. W.; van Gersheim, W.; Martens, F. M.; van der Kerk, S. M. *Tetrahedron* **1986**, *42*, 975-992.

(19) Carlson, B. W.; Miller, L. L. *J. Am. Chem. Soc.* **1985**, *107*, 479-485.

(20) Lai, C. C.; Colter, A. K. *J. Chem. Soc., Chem. Commun.* **1980**, 1115-1116.

(21) Powell, M. F.; Wu, J. C.; Bruice, T. C. *J. Am. Chem. Soc.* **1984**, *106*, 3850-3856. Sinha, A.; Bruice, T. C. *J. Am. Chem. Soc.* **1984**, *106*, 7291-7292.

(22) Carlson, B. W.; Miller, L. L. *J. Am. Chem. Soc.* **1983**, *105*, 7453-7454. Carlson, B. W.; Miller, L. L.; Neta, P.; Grodkowski, J. *J. Am. Chem. Soc.* **1984**, *106*, 7233-7239. Miller, L. L.; Valentine, J. R. *J. Am. Chem. Soc.* **1988**, *110*, 3982-3989.

(23) Fukuzumi, S.; Kondo, Y.; Tanaka, T. *J. Chem. Soc., Perkin Trans. 2* **1984**, 673-679. Bunting, J. W.; Stefanidis, D. *J. Org. Chem.* **1986**, *51*, 2060-2067.

(24) Fukuzumi, S.; Koumitsu, S.; Hironaka, K.; Tanaka, T. *J. Am. Chem. Soc.* **1987**, *109*, 305-316.

(25) Bernasconi, C. F.; Wang, H. *J. Am. Chem. Soc.* **1977**, *99*, 2214-2221.

(26) Colter, A. K.; Saito, G.; Sharom, F. J.; Hong, A. P. *J. Am. Chem. Soc.* **1976**, *98*, 7833-7835. Colter, A. K.; Saito, G.; Sharom, F. J. *Can. J. Chem.* **1977**, *55*, 2741-2751.

(27) Colter, A. K.; Lai, C. C.; Williamson, T. W.; Berry, R. E. *Can. J. Chem.* **1983**, *61*, 2544-2551.

(28) Murray, C. J.; Webb, T. *J. Am. Chem. Soc.* **1991**, *113*, 7426-7427.

(29) (a) Fukuzumi, S.; Ishikawa, M.; Tanaka, T. *J. Chem. Soc., Perkin Trans. 2* **1989**, 1811-1821. (b) Fukuzumi, S.; Mochizuki, S.; Tanaka, T. *J. Am. Chem. Soc.* **1989**, *111*, 1497-1499.

(30) Chambers, J. Q. In *The Chemistry of the Quinoid Compounds*; Patai, S.; Rappoport, Z., Eds.; Wiley-Interscience: New York, NY, 1988; Vol. 2, Part 1, Chapter 12. Rich, P. R.; Bendall, D. S. *Biochim. Biophys. Acta* **1980**, *592*, 506-518. Bailey, S. I.; Ritchie, I. M.; Hewgill, F. R. *J. Chem. Soc., Perkin Trans. 2* **1983**, 645-652. Laviron, E. *J. Electroanal. Chem.* **1984**, *169*, 29-46.

(31) Patel, K. B.; Willson, R. L. *Faraday Trans. 1* **1973**, *69*, 814-825. Veltwisch, D.; Asmus, K.-D. *J. Chem. Soc., Perkin Trans. 2* **1982**, 1147-1152.

(32) Hapiot, P.; Moiroux, J.; Savéant, J.-M. *J. Am. Chem. Soc.* **1990**, *112*, 1337-1343.

**Table I.** Third-Order Rate Constants  $k_{AL}^L$  for General Acid Catalysis of the Reduction of *p*-Benzoquinone by 10-Methylacridan<sup>a</sup>

catalyst	$pK_a^{AH}$	$k_{AH}^H, M^{-2} s^{-1}$	$k_{AD}^H, M^{-2} s^{-1}$	$k_{AH}^D, M^{-2} s^{-1}$	$k_{AD}^D, M^{-2} s^{-1}$
$L_2O^+$	-1.74	6800	11000	3600	
CNCH <sub>2</sub> COOH	2.23	321		204	
CICH <sub>2</sub> COOL	2.70	101	50.4	62.4	36.0
CH <sub>3</sub> OCH <sub>2</sub> COOL	3.40	26.8	18.3		
HOCH <sub>2</sub> COOH	3.64	15.7			
CICH <sub>2</sub> CH <sub>2</sub> COOL	3.93	8.70	3.08	6.19	2.07
CH <sub>3</sub> COOL	4.65	2.97	2.41	2.01	1.55
(CH <sub>3</sub> ) <sub>2</sub> AsO <sub>2</sub> L	6.16	0.72		0.61	
L <sub>2</sub> O	15.74	0.57/55	0.65/55	0.075/55	

<sup>a</sup>In 3% (v/v) ethanol-water at 25 °C, 1 M ionic strength (KCl). The superscript refers to the substrate isotope transferred, and the subscript refers to the general acid catalyst (AL), lyonium ion (L<sup>+</sup>), or solvent (w).

involving partially rate-limiting formation and breakdown of the (1-H<sub>2</sub><sup>++</sup>,QH<sup>-</sup>) radical pair, and (3) constant substrate kinetic isotope effects (KIE)  $k_{AL}^H/k_{AL}^D = 1.5 \pm 0.1$  in water (L = <sup>1</sup>H) or deuterium oxide (L = <sup>2</sup>H) that show both substrate and solvent isotopic substitutions affect the same rate-limiting transition state. These results confirm the conclusion that correlation of the log of the rate constants for hydride transfer with one-electron reduction potentials of acceptors<sup>29</sup> does not provide a reliable criterion for distinguishing between one-step hydride transfers and SET mechanisms.<sup>14,21</sup>

### Experimental Section

**Materials.** 10-Methylacridan, 1-H<sub>2</sub>, was prepared according to the procedure of Colter et al.<sup>26</sup> and was recrystallized from 95% EtOH. [<sup>9-<sup>2</sup>H<sub>2</sub>]-10-Methylacridan, 1-D<sub>2</sub>, was a gift from Professor M. M. Kreevoy. It was shown to be >98.8% deuterated using 500-MHz <sup>1</sup>H NMR spectroscopy. *p*-Benzoquinone (Q) was purified by sublimation. Solutions of *p*-benzoquinone were prepared fresh daily and shielded from light. Ethanol-*O-d* (99% D) and deuterium oxide (D<sub>2</sub>O; 99.9 atom % D) were obtained from Isotec, Inc. Methoxyacetic acid was purified by distillation. Cyanoacetic, chloroacetic, chloropropionic, and cacodylic acids were recrystallized before use. All other materials were of reagent grade and were used without further purification.</sup>

**Methods.** Reactions were carried out in 3% ethanol-water (v/v) at 25 °C and ionic strength 1.0 maintained with potassium chloride. Kinetic data were obtained under pseudo-first-order reaction conditions with at least a 40-fold excess of *p*-benzoquinone. Solution pH and pD were measured with an Orion Model 701A pH meter and a Radiometer GK2321C combination electrode thermostated at 25 °C. The reactions were initiated by injecting 2–4 μL of a 0.015 M stock solution of 1-L<sub>2</sub> in ethanol into 3 mL of buffer solution containing 0.15–2 mM *p*-benzoquinone.

**Kinetics.** Rate constants were determined by monitoring the increase in the absorbance of oxidized 10-methylacridinium ion (1-L<sup>+</sup>) at 358 nm using a Hitachi U-2000 or Hewlett Packard 8452A diode array spectrophotometer with a UV filter for wavelengths below 300 nm. Plots of absorbance against time were fit by a nonlinear least-squares fitting routine<sup>33</sup> to eq 3 that describes two widely separated observed rate constants  $k_1$  and  $k_2$ .<sup>34</sup>

$$A_t = A_0 + \Delta A_1(1 - \exp(-k_1 t)) + \Delta A_2(-k_2 t) \quad (3)$$

In eq 3,  $A_t$  is the measured absorbance at time  $t$ ,  $A_0$  is the initial absorbance,  $k_1$  and  $\Delta A_1$  are the observed rate constant and amplitude for the fast phase, respectively, and  $\Delta A_2 k_2$  describes a slightly sloping infinite line. Although the slow process  $k_2$  was not investigated in detail, it is consistent with the known photochemical instability of *p*-benzoquinone in water.<sup>35</sup> The slow process is not due to contamination of 1-L<sub>2</sub> by trace amounts of acridan<sup>36</sup> as HPLC analysis of 1-H<sub>2</sub> showed no traces of impurities. Photolysis of 10-methylacridan with high-intensity UV light is known to yield the radical cation 1-H<sub>2</sub><sup>++</sup> and radical 1-H<sup>•</sup> by proton loss.<sup>37</sup> Control experiments in the absence of Q showed that 1-H<sub>2</sub> is stable under the reaction conditions used. Bubbling dry argon through

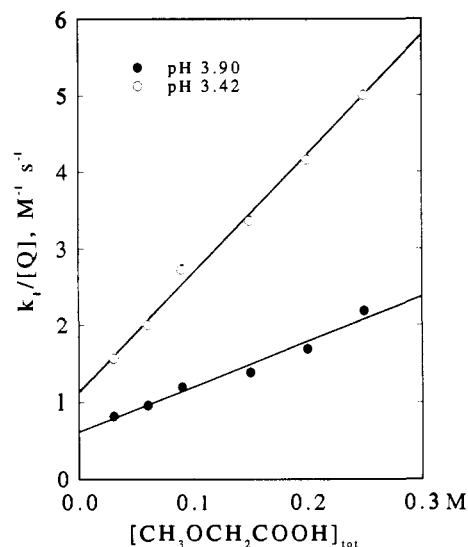


**Figure 1.** Plot of the dependence of  $k_1/[Q]$  on the concentration of methoxyacetic acid for reduction of *p*-benzoquinone by 10-methylacridan in 3% ethanol-water (v/v) at 25 °C and ionic strength 1.0 (KCl): (O) pH 3.42; (●) pH 3.90.

the samples had not effect on the  $k_1$  process. The amplitude of the slow process never amounted to more than a few percent of the overall absorbance change.

Solvent and substrate deuterium isotope effects were determined from measurements in protium and deuterium oxide solutions using identical buffer compositions. Parallel experiments were usually carried out on the same day. The value of pD was obtained by adding 0.40 to the observed pH of the solutions in D<sub>2</sub>O.<sup>38</sup>

**Calculated Brønsted Curves.** Brønsted slopes were statistically corrected for the number of acid and base sites on the catalyst as described by Bell.<sup>39</sup> Theoretical Brønsted curves for diffusion-controlled trapping of the semiquinone radical anion were calculated from eq 4 in which the

$$k_{AH} = \frac{K_e k_a k_p k_b}{k_p k_b + k_{-a} k_b + k_{-a} k_p} \quad (4)$$

rate constants are defined in eq 7 with  $K_e = k_{et}/k_{-et}$ . Rate constants for diffusion-controlled steps are similar to those reported by Eigen with a 15-fold positive deviation for hydronium ion.<sup>40</sup> The theoretical curve shown as the dashed line in Figure 4 was calculated with  $pK_a^{QH^•} = 4.1$ ,  $\log k_{\pm p} = 11 \pm 0.5 \Delta pK$ ,  $k_b = k_{-a} = 10^{11} s^{-1}$ , and  $K_e k_a = 1.5 \times 10^2 M^{-2} s^{-1}$ .

### Results

**Kinetics: pH and Buffer Dependence.** The reduction of excess *p*-benzoquinone, Q, by 10-methylacridan in the presence of buffer acids, AH, follows the rate law

$$k_1 = (k_0 + k_{cat}[AH]_{tot})[Q] \quad (5)$$

in which  $k_0$  and  $k_{cat}$  are rate constants for the buffer-independent

(33) The data were fit using Enzfitter software by Biosoft (J. Leatherbarrow, Elsevier: New York, 1987).

(34) Bernasconi, C. F. *Relaxation Kinetics*; Academic: New York, 1976; pp 142–143.

(35) Hashimoto, S.; Kano, K.; Okamoto, H. *Bull. Chem. Soc. Jpn.* **1972**, *45*, 966.

(36) Bunting, J. W.; Chew, V. S. F.; Chu, G.; Fitzgerald, N. P.; Gunasekara, A.; Oh, H. T. P. *Bioorg. Chem.* **1984**, *12*, 141–157.

(37) Shukla, D.; de Rege, F.; Wan, P.; Johnston, L. J. *J. Phys. Chem.* **1991**, *95*, 10240–10246.

(38) Glasoe, P. K.; Long, F. A. *J. Phys. Chem.* **1960**, *64*, 188–191.

(39) Bell, R. P. *The Proton in Chemistry*, 2nd ed.; Cornell University Press: Ithaca, NY, 1976; pp 197–198.

(40) Eigen, M. *Angew. Chem., Int. Ed. Engl.* **1964**, *4*, 1–19.

**Table II.** Substrate and Solvent Kinetic Isotope Effects for General Acid Catalysis of the Reduction of *p*-Benzoquinone by 10-Methylacridan<sup>a</sup>

catalyst	pK <sub>a</sub> <sup>AH</sup>	solvent isotope effects <sup>b</sup>		substrate isotope effects <sup>b,c</sup>	
		k <sub>AH</sub> <sup>H</sup> /k <sub>AD</sub> <sup>H</sup>	k <sub>AH</sub> <sup>D</sup> /k <sub>AD</sub> <sup>D</sup>	k <sub>AH</sub> <sup>H</sup> /k <sub>AL</sub> <sup>D</sup>	k <sub>AD</sub> <sup>H</sup> /k <sub>AD</sub> <sup>D</sup>
L <sub>3</sub> O <sup>+</sup>	-1.74	0.62 ± 0.1		1.9 ± 0.1	
CNCH <sub>2</sub> COOH	2.23			1.57 ± 0.11	
ClCH <sub>2</sub> COOL	2.70	2.01 ± 0.20	1.73 ± 0.20	1.62 ± 0.19	1.40 ± 0.13
CH <sub>3</sub> OCH <sub>2</sub> COOL	3.40	1.6 ± 0.5			
ClCH <sub>2</sub> CH <sub>2</sub> COL	3.93	2.82 ± 0.17	2.99 ± 0.19	1.41 ± 0.09	1.49 ± 0.10
CH <sub>3</sub> COOL	4.65	1.23 ± 0.07	1.32 ± 0.13	1.48 ± 0.11	1.56 ± 0.13
(CH <sub>3</sub> ) <sub>2</sub> AsO <sub>2</sub> H	6.16			1.17 ± 0.18	
L <sub>2</sub> O	15.74	0.8 ± 0.1		7.6 ± 0.1	

<sup>a</sup>In 3% (v/v) ethanol-water at 25 °C, 1 M ionic strength (KCl). <sup>b</sup>The superscript refers to the substrate isotope transferred, and the subscript refers to the general acid catalyst (AL), lyonium ion (L<sup>+</sup>), or solvent (w). <sup>c</sup>The substrate isotope effects are the product of primary and secondary kinetic isotope effects; see text.

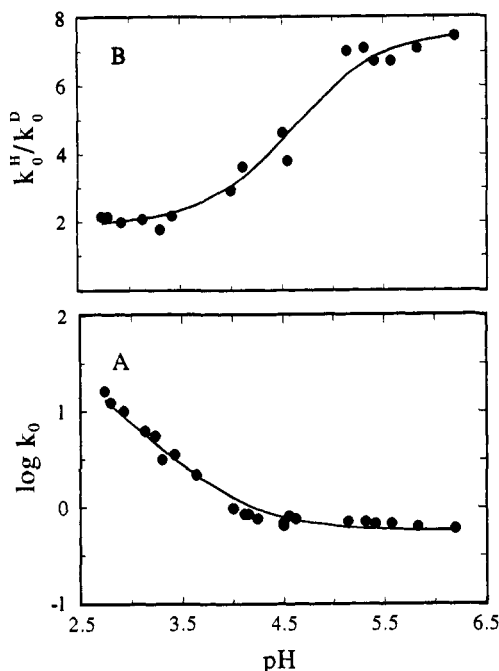


**Figure 2.** (A) Plot of the dependence of the second-order rate constants  $k_0$  on pH for the reduction of *p*-benzoquinone by 10-methylacridan in 3% ethanol-water (v/v) at 25 °C and ionic strength 1.0. The solid line is a fit of the data to eq 6 with  $k_w = 0.57 \text{ M}^{-1} \text{ s}^{-1}$  and  $k_{\text{H}^+} = 6.8 \times 10^3 \text{ M}^{-2} \text{ s}^{-1}$ . (B) Plot of the dependence of the substrate isotope effect  $k_0^{\text{H}}/k_0^{\text{D}}$  on pH.

and buffer-catalyzed reactions, respectively. Second-order rate constants for the buffer-independent reaction,  $k_0$ , are given by eq 6

$$k_0 = k_w + k_{\text{H}^+}[\text{H}^+] \quad (6)$$

where the rate constants  $k_w$  and  $k_{\text{H}^+}$  are for the "water"-catalyzed and hydronium ion catalyzed reduction, respectively, at ionic strength 1.0 M.

The third-order rate constants for buffer catalysis,  $k_{\text{cat}}$ , were obtained from the least-squares slopes of plots of  $k_1/[Q]$  against total buffer concentration as shown in Figure 1 for catalysis by methoxyacetic acid in water. Typically plots according to eq 5 were linear up to 0.5 M buffer. All of the buffers showed catalysis by the acidic but not the basic form of the buffer so that  $k_{\text{cat}} = k_{\text{AH}}^{\text{H}}/f_{\text{AH}}$ , where  $f_{\text{AH}}$  is the fraction of free buffer acid. Third-order rate constants for general acid catalysis  $k_{\text{AH}}^{\text{H}}$  are summarized in Table I.<sup>41</sup>

Buffer-independent rate constants were obtained from the intercepts of the plots in Figure 1 and were fit to the pH-rate profile shown in Figure 2A with  $k_w^{\text{H}} = 0.57 \text{ M}^{-1} \text{ s}^{-1}$  and  $k_{\text{H}^+}^{\text{H}} = 6.8 \times 10^3 \text{ M}^{-2} \text{ s}^{-1}$ . Similar data obtained in deuterium oxide (data not

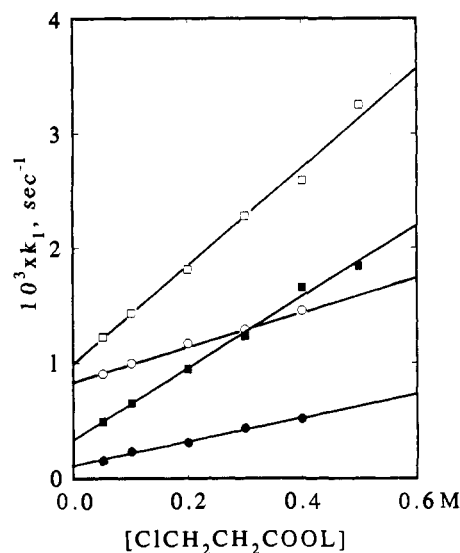
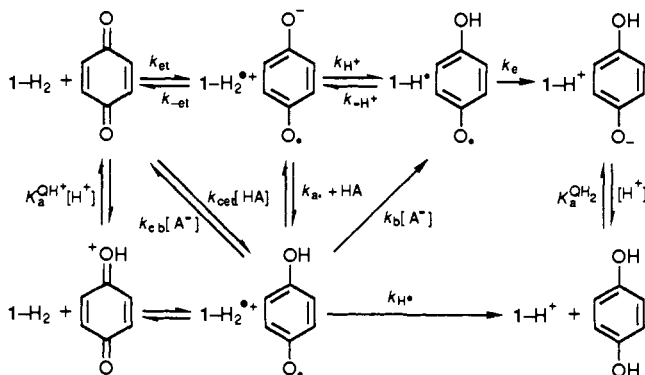


**Figure 3.** Plot of the dependence of the observed rate constant  $k_1$  on chloropropionic acid concentration in H<sub>2</sub>O (□, ■) and D<sub>2</sub>O (○, ●) for reduction of 1.0 mM *p*-benzoquinone by [9-*L*]-10-methylacridan in 3% ethanol-water (v/v) at 25 °C and ionic strength 1.0 (KCl). The open symbols are for 1-H<sub>2</sub> and the closed symbols are for 1-D<sub>2</sub>.

#### Scheme I



shown) yield  $k_0^{\text{D}} = 0.65 \text{ M}^{-1} \text{ s}^{-1}$  and  $k_{\text{H}^+}^{\text{D}} = 1.1 \times 10^4 \text{ M}^{-2} \text{ s}^{-1}$ . Values of  $k_0$  and  $k_{\text{cat}}$  in water and deuterium oxide are summarized in the supplementary material, Table S1.

**Solvent and Substrate Deuterium Isotope Effects.** Solvent and substrate KIEs were generally measured in comparable buffer solutions on the same day. Figure 2B shows the change in the substrate isotope effect on the buffer-independent rate constants  $k_0$  from a limiting value of  $k_{\text{H}^+}^{\text{H}}/k_{\text{H}^+}^{\text{D}} = 1.9$  at low pH to  $k_{\text{H}^+}^{\text{H}}/k_{\text{H}^+}^{\text{D}} = 7.6$  at high pH. Figure 3 shows a typical determination of solvent KIEs  $k_{\text{AH}}^{\text{H}}/k_{\text{AD}}^{\text{H}}$  and substrate KIEs  $k_{\text{AL}}^{\text{H}}/k_{\text{AL}}^{\text{D}}$  for general acid catalysis (where L refers to the isotopic identity of the substrate or solvent, respectively) for catalysis by chloropropionic acid. Values of the third-order rate constants  $k_{\text{AL}}^{\text{H}}$  are summarized in Table I and the KIEs are summarized in Table II, including

(41) For the rate constants listed in Table I, the superscript refers to the substrate isotope transferred, and the subscript refers to the general acid catalyst (AL), lyonium ion (L<sup>+</sup>), or solvent (w).

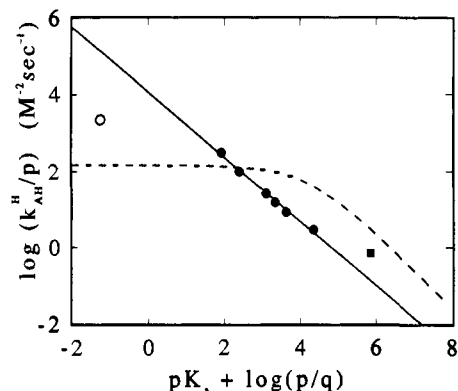


**Figure 4.** Brønsted plot for general acid catalysis of the reduction of *p*-benzoquinone by 10-methylacridan. The solid circles (●) represent substituted acetic acid catalysts, the solid square (■) represents cacodylic acid, and the open circle (○) represents hydronium ion. The solid line is drawn with a slope of  $\alpha = 0.85$  through the points for the RCOOH catalysts. The dashed line is calculated for a diffusion-controlled trapping of the semiquinone radical anion ( $pK_a^{QH^{\bullet}} = 4.1$ ) according to eq 4 as described in the Experimental Section.

isotope effects for the “water” and lyonium ion reactions.

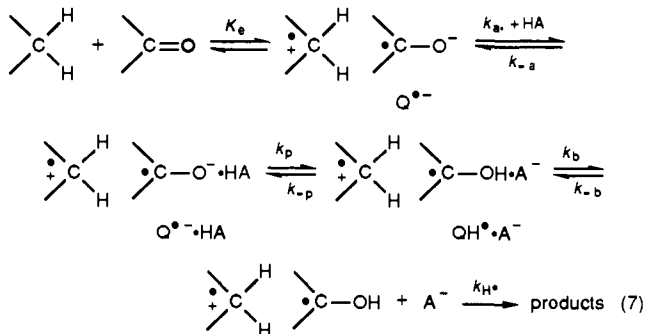
### Discussion

**SET Mechanisms.** The specific acid-catalyzed reduction of *p*-benzoquinone by 10-methylacridin in 20% ethanol–water (v/v) has been suggested to occur by the SET mechanism outlined in Scheme I.<sup>29</sup> In Scheme I, the upper  $k_{et}$ ,  $k_{H^+}$ ,  $k_e$  pathway corresponds to the uncatalyzed reaction at  $pH > pK_a^{QH^{\bullet}} = 4.1$  involving an intermediate radical anion–radical cation pair with the proton transfer step rate-limiting. This mechanism has previously been ruled out by several workers.<sup>19,27</sup>

The increase in the rate of the reaction at  $pH < 4$  has been suggested as evidence for formation of the semiquinone radical,  $QH^{\bullet}$ . This intermediate may be generated either directly by acid-catalyzed one-electron transfer,  $k_{cat}[HA]$ , or by trapping of the semiquinone radical anion,  $Q^{\bullet-}$ , by added acid,  $k_a[HA]$ . Hydrogen atom transfer from  $1-H_2^{++}$  to  $QH^{\bullet}$ ,  $k_{H^+}$ , forms the products 10-methylacridinium ion,  $1-H^+$ , and hydroquinone,  $QH_2$ . The log of the second-order rate constants for hydride transfer from 10-methylacridin correlates with the one-electron reduction potentials of substituted *p*-benzoquinones at both acidic and neutral pH values.<sup>29</sup> This has been suggested as further evidence for the mechanism outlined in Scheme I.

However, the interpretation of the experimental data in terms of the SET mechanism shown in Scheme I can be excluded by the following:

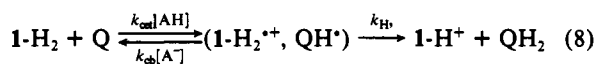
(1) The Brønsted plot for general-acid catalysis of the reduction of *p*-benzoquinone by 10-methylacridin in 3% ethanol–water (v/v) at ionic strength 1.0 M (KCl) is shown in Figure 4. The straight line slope drawn through the points for carboxylic acids corresponds to a Brønsted  $\alpha = 0.85$ . The dashed line in Figure 4 is calculated for a “trapping” mechanism outlined in more detail as eq 7 where  $k_a$  and  $k_b$  are diffusional steps and  $k_p$  is a proton transfer step. In eq 7, the initially formed radical ion pair



$1-H_2^{++}Q^{\bullet-}$  will revert to reactants with a rate constant  $k_{-et}$  if it

is not trapped by protonation,  $k_p$ , after encounter with an acid,  $k_a[HA]$ , followed by rapid hydrogen atom transfer,  $k_{H^+}$ , within the  $1-H_2^{++}QH^{\bullet}$  encounter complex. The trapping mechanism will follow an “Eigen curve” with a break at  $pK_a = 4.1$  corresponding to the  $pK_a$  of the semiquinone radical.<sup>31</sup> The dashed line in Figure 4 shows an “Eigen curve” with a break at  $pK_a = 4.1$  calculated as described in the Experimental Section that is clearly inconsistent with the experimental data. In addition, the mechanism of eq 7 predicts a maximum in the solvent KIE at  $\Delta pK_a \approx 0.5$ .<sup>42</sup> The solvent KIEs summarized in Table II are small and may show a slight mechanism near  $pK_a \approx 4$ , but no definite trend is observed. The absence of a break in the Brønsted plot and the small solvent KIEs show that the trapping mechanism is inconsistent with the experimental data.

(2) Alternatively, at  $pH < pK_a^{QH^{\bullet}}$ , Scheme I reduces to eq 8



from which application of the steady-state approximation yields eq 9. There is no evidence for curvature in the buffer plots such

$$k_{AH}^H = \frac{k_{H^+} k_{cat} [AH]}{k_{H^+} + k_{cb} [A^-]} \quad (9)$$

as shown in Figures 1 and 3 up to 0.5 M total buffer. This is inconsistent with the expected change in rate-limiting step from acid catalyzed electron transfer,  $k_{cat}$ , to hydrogen atom transfer,  $k_{H^+}$ , with increasing buffer concentration according to eq 9. A lower limit for the rate constant ratio  $k_{cb}/k_{H^+} < 0.1 \text{ M}^{-1}$  can be estimated from a fit of the data in Figure 1 at  $pH 3.42$  to eq 9. The absence of buffer curvature requires that acid catalyzed electron transfer be rate-limiting if the mechanism of eq 8 holds. However, the observed substrate kinetic isotope effect  $k_{AL}^H/k_{AL}^D = 1.5 \pm 0.1$  for substituted acetic acid catalysts in water requires that transfer of the substrate hydrogen be partially rate-limiting.<sup>43</sup> Both of these conditions cannot be met at the same time and so we conclude that the mechanism of eq 8 is excluded. In addition, general acid catalysts of electron transfer is not expected in the case of more basic catalysts with  $pK_a > 4$ , according to the “libido rule” of Jencks,<sup>44</sup> because proton transfer from the catalyst to a transition state less basic than  $Q^{\bullet-}$  is thermodynamically unfavorable.

In principle, the Brønsted plot in Figure 4 is consistent with a SET mechanism involving acid catalyzed one-electron transfer,  $k_{cat}[H^+]$ , followed by a rate-limiting general base catalyzed deprotonation of  $1-H_2^{++}$ ,  $k_b[A^-]$  in Scheme I, with a Brønsted  $\beta = 1 - \alpha = 0.15$ . This is similar to the  $\beta$  value of 0.2 determined by Sinha and Bruce<sup>21</sup> for the unambiguous one-electron oxidation of 10-methylacridin by the relatively strong oxidant  $Fe(CN)_6^{3-}$  that shows a substrate KIE  $k^H/k^D = 4.4$  for acetate ion catalysis. However, the multiple isotope effects summarized in Table II provide evidence against this SET pathway as described below.

**Multiple Isotope Effects.** The multiple isotope effect (MIE) method was developed by Hermes et al.<sup>45</sup> and Belasco et al.<sup>46</sup> to distinguish between stepwise and concerted mechanisms in enzyme catalyzed reactions. Briefly, the method involves selective deuteration at one site in a molecule (e.g. a C–H bond-breaking site) followed by an examination of how the magnitude of the kinetic

(42) Yang, C. C.; Jencks, W. P. *J. Am. Chem. Soc.* **1988**, *110*, 2972–2973.

(43) In principle, the substrate KIEs  $k_{AL}^H/k_{AL}^D$  could represent a normal secondary isotope effect on the electron transfer rate constant,  $k_{cat}$ , due to a decrease in the 9-C–L bending force constant upon going from  $1-H_2$  to the radical cation-like transition state. The magnitude of this isotope effect is expected to be less than 1.2 based on the secondary kinetic isotope effect  $k_{HH}/k_{DD} = 1.05 \pm 0.13$  for the one-electron oxidation of *N*-propyl-1,4-dihydroxycotinamide by  $Fe(CN)_6^{3-}$ .<sup>21</sup>

(44) Jencks, W. P. *J. Am. Chem. Soc.* **1972**, *94*, 4731–4732.

(45) Hermes, J. D.; Roeske, C. A.; O’Leary, M. H.; Cleland, W. W. *Biochemistry* **1982**, *21*, 5106–5114. Cleland, W. W. In *Enzyme Mechanism from Isotope Effects*; Cook, P. F., Ed.; Chemical Rubber Company: Boca Raton, FL, 1991; pp 247–268.

(46) Belasco, J. G.; Albery, W. J.; Knowles, J. R. *J. Am. Chem. Soc.* **1983**, *105*, 2475–2477.

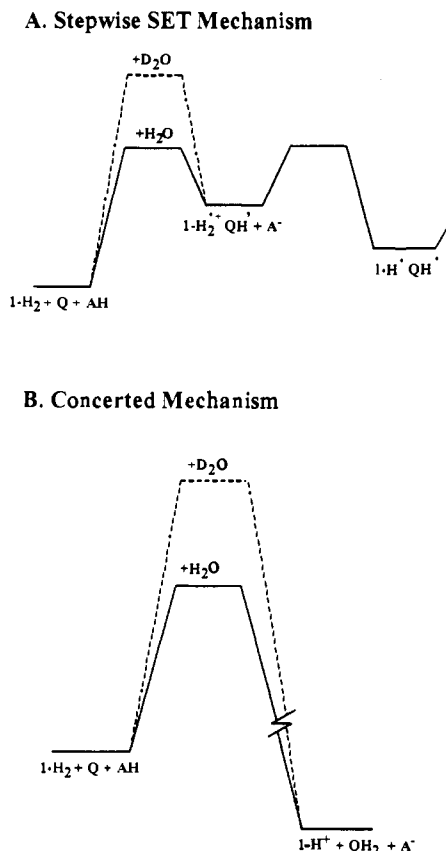


**Figure 5.** Schematic free energy diagram for (A) a stepwise mechanism involving acid catalyzed electron transfer followed by general-base catalyzed deprotonation of  $1\text{-H}_2^+$  and (B) a concerted mechanism involving general-acid catalysis of hydride transfer. The dashed line represents the effective increase in the free energy barrier due to deuterium substitution in the solvent.

isotope effect at an alternate, bond-making site is affected. Figure 5 illustrates how the MIE method can be used to distinguish between a stepwise mechanism (a) involving acid catalyzed electron transfer followed by general base catalyzed deprotonation of  $1\text{-H}_2^{2+}$  and a concerted mechanism (b) involving a one-step hydride transfer with proton donation to the carbonyl oxygen by the acid catalyst. For the stepwise mechanism, the substrate KIE on the deprotonation of the radical cation by buffer bases will be partially "masked" in  $\text{D}_2\text{O}$ , due to the solvent KIE on the initial electron transfer step. For the concerted reaction, only one step is isotopically sensitive so that the substrate KIE will be independent of the isotopic identity of the solvent.<sup>47</sup> The data summarized in Table II show that, within experimental error, the substrate KIEs are independent of the isotopic identity of the solvent, thus confirming the one-step concerted mechanism for acid catalyzed hydride transfer.

It should be noted that the observed substrate KIE is the product of secondary and primary effects. Extensive studies of primary and secondary isotope effects in hydride transfer reactions have shown that the reaction-coordinate motion is coupled at both the secondary and primary (transferred) hydrogens.<sup>13</sup> This coupled motion can lead to exalted secondary kinetic isotope effects and diminished primary kinetic isotope effects.<sup>48</sup> This may be one factor that accounts for the small magnitude of the substrate kinetic isotope effects for general-acid catalysis.

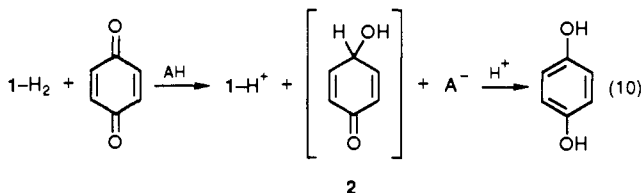
**Concerted Hydride and Proton Transfer.** Having ruled out several reasonable mechanisms involving one-electron transfer intermediates, we conclude that the reaction mechanism is a single

(47) This analysis assumes (a) that the two isotopic sites behave independently and (b) other non-isotopically sensitive steps are not partially rate-limiting.

(48) Huskey, W. P.; Schowen, R. L. *J. Am. Chem. Soc.* **1983**, *105*, 5704–5706.

step hydride transfer catalyzed by added general acids. Several mechanistic questions arise in this context: (1) Is the hydride ion equivalent delivered to the carbonyl carbon or oxygen? (2) Does acid catalysis of these reactions represent a proton "in-flight" or simply hydrogen-bond stabilization of the transition state?

Colter et al.<sup>26</sup> have established that the hydride is not delivered to the C-2 or C-3 carbons on the basis of the absence of deuterium incorporation into the product  $\text{QH}_2$  when Q is reduced by  $1\text{-HD}$  in 90% acetonitrile–water. In principle, the mechanism outlined in eq 10 could account for the absence of deuterium incorporation



into the product as well as the well-known propensity of hydride ions to add to carbon over oxygen. The initial unstable product, 4-hydroxycyclohexa-2,5-dienone (2), should enolize rapidly to the more stable hydroquinone product. Similar cyclohexa-2,5-dienone intermediates have been observed spectroscopically on the millisecond time scale in the bromination of phenol.<sup>49</sup>

Alternatively a mechanism involving hydride transfer to the carbonyl oxygen with proton transfer to the second oxygen to yield the hydroquinone product  $\text{QH}_2$  directly cannot be excluded.<sup>19</sup> In the following discussion, we shall assume that hydride ion and proton are delivered to the same carbonyl group according to eq 10.

The solvent KIEs apparently show a maximum isotope effect of 3 at  $\text{pK} \approx 4$ , corresponding to chlorpropionic acid as a catalyst. Similar solvent isotope effect maxima with  $k_{\text{HOH}}/k_{\text{DOD}} = 3\text{--}4$  have been observed for oxygen to oxygen hydron transfers.<sup>8</sup> The relatively small magnitudes of the solvent and substrate KIEs for general acid catalysis may represent a coupling between the motion of heavy atoms with proton transfer in the transition state.<sup>50</sup> Alternatively, the small solvent KIEs may represent "solvation catalysis" with the proton in a hydrogen-bonded potential well in the transition state.<sup>51</sup> This is consistent with the large Brønsted  $\alpha$  value of 0.85 that suggests a large degree of proton transfer from the  $\text{RCOOH}$  catalyst to the carbonyl oxygen in the transition state.

There is some evidence for an early transition state for hydride transfer from changes in rate constants with changes in the electron affinity of substituted benzoquinones. This is consistent with concerted nucleophilic attack of the hydride ion coupled with proton transfer. A detailed analysis is not possible now but a crude measure of the amount of hydride transfer can be estimated from a Brønsted-type plot of  $\log k_{\text{AH}}$  against the log of the relative change in the overall equilibrium constant for reactions of *p*-benzoquinone and methyl-substituted benzoquinones catalyzed by hydronium ion<sup>29,52</sup> and chlorpropionic acid (data not shown).<sup>52</sup> The slopes of the correlations are  $\rho_n = 0.2\text{--}0.3$ . This is consistent with the small magnitude of the substrate KIEs that indicate only a small loss in zero-point energy upon going from the ground state to the transition state. A slightly larger value of  $\rho_n = 0.5$  has been reported by Carlson and Miller<sup>19</sup> for the uncatalyzed reduction of substituted *p*-benzoquinones by NADH in water.

(49) Tee, O. S.; Iyengar, N. R. *J. Am. Chem. Soc.* **1985**, *107*, 455–459.

(50) Coleman, C. A.; Murray, C. J. *J. Am. Chem. Soc.* **1991**, *113*, 1676–1684.

(51) Swain, C. G.; Kuhn, D. A.; Schowen, R. L. *J. Am. Chem. Soc.* **1965**, *87*, 1553–1561.

(52) The ratio of equilibrium constants for reduction of *p*-benzoquinone and substituted benzoquinones can be calculated from the two-electron reduction potentials in water<sup>30</sup> according to  $\log(K/K_0) = n\Delta E^\circ/0.059$ . The corresponding rate constant ratios for hydronium ion catalysis in 20% ethanol–water are estimated from the data for *p*-benzoquinone and 2-methyl-*p*-benzoquinone in Figure 2 of ref 29a. For chlorpropionic acid catalysis in 3% (v/v) MeCN–water, the third order rate constant for reduction of 2,5-dimethylbenzoquinone is  $k_{\text{AH}}^{\text{H}} = 0.70$  (unpublished results).

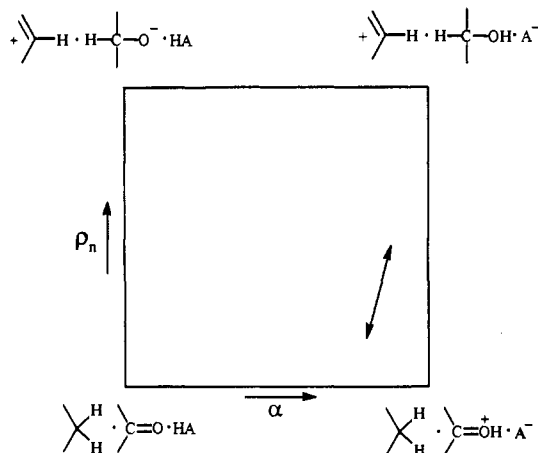


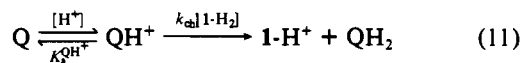
**Figure 6.** Reaction coordinate–energy diagram illustrating the coupling between hydride and proton transfer in the reduction of substituted *p*-benzoquinones by 10-methylacridan catalyzed by general acids. The *x* axis is defined by  $\alpha$  which measures proton transfer and the *y* axis is defined by  $\rho_n$  as described in the text. The solid arrow describes the “direction” of the transition state and indicates only weak coupling between hydride and proton transfer.<sup>53</sup>

The structure–reactivity behavior can be illustrated using the three-dimensional reaction coordinate–energy diagram shown in Figure 6. The *x* axis is defined by the Brønsted coefficient  $\alpha$  that describes proton transfer from the acid catalyst, and the *y* axis is defined by the normalized  $\rho$  value,  $\rho_n$ , that describes C–H bond formation in the transition state. The position of the transition state on the diagram is shown with values of  $\alpha = 0.85$  and  $\rho_n = 0.25$ . The direction of the transition state is not known with certainty but is shown in a largely vertical direction indicating a weakly coupled or hydrogen bonded transition state.<sup>53</sup>

Our experimental results show surprising similarities with the AM1 calculated transition-state structure for reduction of formaldehyde by dihydropyridine catalyzed by imidazole.<sup>54</sup> For example, the position of the transition state with respect to hydride and proton transfer is highly asynchronous with proton transfer well ahead of hydride transfer in the transition state. Similarly, the small magnitude of the calculated hydron transfer isotope effects ( $k_H/k_D \approx 2.3$ ) and hydride transfer isotope effects ( $k_H/k_D = 1.6\text{--}2.0$ ) reflects a kinetic coupling of both proton and hydride transfer along the reaction coordinate.

**Solvent Assisted Pathways.** The third-order rate constant for hydronium ion catalysis is 60-fold smaller than predicted by the Brønsted plot for RCOOH catalysts in Figure 4. This suggests a different mechanism for catalysis by hydronium ion.

It has been suggested<sup>29</sup> that hydronium ion catalysis must occur by a SET mechanism because equilibrium protonation of Q to form protonated benzoquinone, QH<sup>+</sup>, followed by rate-limiting hydride transfer,  $k_{ch}$  (eq 11), would require a value for the second-order rate constant  $k_{ch}$  that exceeds the diffusion-controlled



limit. This conclusion is based upon an estimate of the  $pK_a$  of protonated benzoquinone ( $pK_a^{QH^+} \approx -7$ ) that has not been directly determined. Palm and others have noted that protonated carbonyl groups give a hydrogen-bonded complex, rather than a fully protonated base, so that it is notoriously difficult to measure the

acidity constants of protonated ketones.<sup>55</sup> A reasonable estimate of  $pK_a^{QH^+} \approx -3$  is based upon the measured  $pK_a = -2.4$  for the conjugate acid of 4,4-dimethylcyclohexa-2,5-dienone<sup>56</sup> and gives  $k_{ch} = k_H + K_a^{QH^+} = (6.8 \times 10^3)(10^3) = 7 \times 10^6 \text{ M}^{-1} \text{ s}^{-1}$ , well below the diffusion limit.

The mechanism of eq 11 is also consistent with the inverse solvent isotope effect  $k_H^H/k_D^H = 0.62$  that is the product of the solvent isotope effect for hydride transfer,  $(k_{ch})_{H_2O}/(k_{ch})_{D_2O} = 1.3$ , and an inverse equilibrium isotope effect on the “acidity constant”,  $K_a^{QH^+}/K_a^{QH^+} = I^2/\phi_{QL} \approx I^2 = 0.48$ , where  $\phi_{QL}$  and  $I = 0.69$  are the fractionation factors for protonated benzoquinone and hydronium ion, respectively. The small solvent KIE on  $k_{ch}$  is consistent with a hydrogen-bonded complex,  $[>C=O \cdots H \cdots OH_2]^+$ , of the carbonyl group of benzoquinone and the solvated proton in the transition state.

Although the available experimental evidence points to the mechanism of eq 11 for hydronium ion catalysis, it is difficult to unambiguously rule out a one-electron pathway through the bottom half of Scheme I for this reaction. This is because the estimated one-electron reduction potential of protonated benzoquinone  $E^\circ(QH^+/QH^+) \approx 0.5 \text{ V}$  in water<sup>57</sup> is similar to  $E^\circ(Fe^{3+}/Fe^{2+}) = 0.46 \text{ V}$  for  $Fe(CN)_6^{3-}$  in water at ionic strength  $0.5 \text{ M}$ <sup>58</sup> that has been shown to react with 10-methylacridan by a SET mechanism.<sup>21</sup> A mechanism for the hydronium ion catalysis, analogous to eq 8, would require both acid-catalyzed electron transfer and hydrogen atom transfer to be partially rate-limiting in order to account for both the inverse solvent KIE and the normal substrate KIE  $k_H^H/k_D^H = 1.9$ . The fractionation factor for the semiquinone radical is not known, but the radical would have to be strongly hydrogen bonded to the solvent in order to give rise to an inverse solvent KIE. The small substrate KIE is consistent with partially rate-limiting hydrogen atom transfer from the radical ion pair  $1-H_2^+ \cdots Q^{\cdot-}$  but is substantially smaller than kinetic isotope effects  $k_H/k_D = 29$  reported for the one-electron oxidation of hydroquinone by QH<sup>+</sup> by polypyridyl–oxo complexes of ruthenium(IV) by proton coupled electron transfer in the reverse direction.<sup>59</sup>

The “water”-catalyzed reaction shows a large substrate kinetic isotope effect  $k_H^H/k_D^H = 7.6$ , but it is smaller than the isotope effect  $k_{HH}/k_{DD} = 14.1$  for the uncatalyzed reaction in acetonitrile.<sup>27</sup> This confirms the decreasing trend in the substrate KIE with increasing water content in acetonitrile–water solvent mixtures reported by Colter et al.<sup>27</sup> The origin of this decrease in KIE in the more polar, hydroxylic solvent is unclear, but it may reflect the increased thermodynamic driving force in more polar solvents. These results are in contrast with the small increase in primary kinetic isotope effects with increasing solvent viscosity for the reduction of 1-benzyl-3-cyanoquinolinium ion by 10-methylacridan.<sup>60</sup> Changes in KIEs with changes in solvent viscosity have been modeled using a three-step model that includes solvent translational and rotational motion and assumes the hydride transfer is a tunneling process. The slightly inverse solvent KIE suggests weak hydrogen bond stabilization of the developing oxyanion (either intermediate  $2^-$  or QH<sup>-</sup>) by the solvent in the transition state. Acid catalysis by water of a class e reaction mechanism is not expected because there is no thermodynamic advantage to protonation of the product oxyanion by water acting as a general acid. The water reaction

(55) Palm, V. A.; Haldna, Ü. L.; Talvik, A. J. *The Chemistry of the Carbonyl Group*; Patai, S., Ed.; Wiley-Interscience: New York, 1966; p 439. Bagno, A.; Lucchini, V.; Scorrano, G. *Bull. Soc. Chim. Fr.* **1987**, 563–572.

(56) Cook, K. L.; Waring, A. J. *J. Chem. Soc., Perkin Trans. 2* **1973**, 84–87.

(57) An estimate of the one-electron reduction potential of protonated benzoquinone,  $E^\circ(QH^+/QH^+) \approx 0.5 \text{ V}$ , can be obtained from  $E^\circ(QH^+/QH^+) = E^\circ(Q/Q^{\cdot-}) + (2.303RT/F) \log(K_a^{QH^+}/K_a^{QH^+})$  with  $E^\circ(Q/Q^{\cdot-}) = 0.081 \text{ V}$ ,  $pK_a^{QH^+} \approx -3$ , and  $pK_a^{QH^+} = 4.1$ . Laviron<sup>56</sup> has estimated  $E^\circ(QH^+/QH^+) = 0.756 \text{ V}$  using  $pK_a^{QH^+} = -7$ .

(58) Hanania, G. I. H.; Irvine, D. H.; Eaton, W. A.; George, P. J. *Phys. Chem.* **1967**, 71, 2022–2030.

(59) Binstead, R. A.; McGuire, M. E.; Dvovetoglou, A.; Seok, W. K.; Roecker, L. E.; Meyer, T. J. *J. Am. Chem. Soc.* **1992**, 114, 173–186.

(60) Kreevoy, M. M.; Kotchevar, A. T. *J. Am. Chem. Soc.* **1990**, 112, 3579–3583.

(53) The direction of the transition state on diagrams such as Figure 4 is defined empirically by changes in multiple structure–reactivity correlations that define the curvatures at the saddle-point (Jencks, W. P. *Chem. Rev.* **1985**, 85, 511–527 and references cited therein). It is important to note that Figure 6 is not a potential-energy surface and the curvatures calculated empirically may bear no relation to reaction-coordinate eigenvectors calculated by quantum-mechanical methods. Experiments are in progress to define the direction of the reaction coordinate using multiple structure–reactivity correlations.

(54) Wilkie, J.; Williams, I. H. *J. Am. Chem. Soc.* **1992**, 114, 5423–5425.



can be described by a vertical reaction coordinate on the left side of Figure 4 that corresponds to a stepwise mechanism.

**Acknowledgment** is made to the donors of the Petroleum Research Fund, administered by the American Chemical Society,

for support of this research.

**Supplementary Material Available:** Table S1 summarizing rate constants  $k_0$  and  $k_{\text{cat}}$  in water and deuterium oxide (4 pages). Ordering information is given on any current masthead page.

## Turnover Control of Photosystem II: Use of Redox-Active Herbicides To Form the $S_3$ State

Jeffrey R. Bocarsly<sup>†</sup> and Gary W. Brudvig\*

Contribution from the Department of Chemistry, Yale University, New Haven, Connecticut 06511. Received March 23, 1992

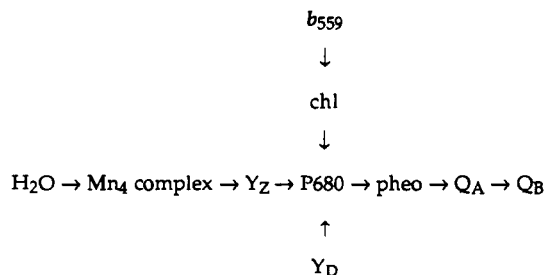
**Abstract:** The  $O_2$ -evolving center of photosystem II, which contains an active-site tetramanganese-oxo cluster, catalyzes the four-electron oxidation of two water molecules to dioxygen, with the concomitant production of four  $H^+$  and four electrons. During catalytic turnover, the manganese-oxo cluster steps through five intermediate oxidation states, which are known as the  $S_i$  states ( $i = 0-4$ ). While methods have been found to manipulate the system into  $S_1$  and  $S_2$  in high yields, efficient production of the  $S_3$  state in good yield at high concentration has not yet been achieved. Previous methods have suffered from the requirement of low protein concentration so that actinic flashes are saturating; the use of temperature to control S-state advancement under continuous illumination, which can lead to S-state scrambling; or the use of herbicides that bind to the  $Q_B$  site and restrict the system to one turnover. We describe here a method for the high-yield production of the  $S_3$  state in highly-concentrated samples of photosystem II, through the use of electron-accepting herbicides which bind to the  $Q_B$  site. Redox-active herbicides can be used, in principle, to limit S-state cycling to any desired number of turnovers, given the appropriate herbicide. This work has fundamental methodological implications not only for the study of photosystem II but also for other multistate redox protein systems.

Photosystem II (PSII) is a multicomponent plant membrane protein complex which utilizes light energy to drive the catalytic oxidation of water.<sup>1</sup> The water-oxidation reaction occurs at an active site containing a tetrameric manganese complex.<sup>2</sup> The manganese complex is the first component in the electron-transfer chain of PSII which consists, in sequence, of a redox-active tyrosine residue ( $Y_Z$ ), the primary chlorophyll electron donor (P680), a pheophytin molecule (pheo), the primary quinone electron acceptor ( $Q_A$ ), and finally a secondary quinone electron acceptor ( $Q_B$ ). A second redox-active tyrosine ( $Y_D$ ), a chlorophyll molecule (chl), and cytochrome  $b_{559}$  are alternate electron donors in PSII. Of these alternate donors, cytochrome  $b_{559}$  has been shown to donate to P680<sup>+</sup> via an intermediary chlorophyll,<sup>3</sup> and  $Y_D$  donates directly to P680<sup>+</sup>.<sup>4</sup> These reactions are summarized in Scheme I.<sup>5</sup>

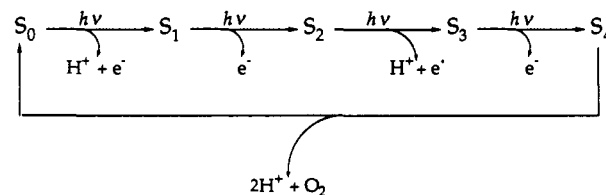
During PSII turnover, the manganese tetramer stores 4 oxidizing equiv produced by the photochemical apparatus of PSII. These oxidizing equivalents are used to oxidize 2 equiv of water to generate four protons and a molecule of dioxygen. Thus, the manganese cluster has five accessible oxidation states through which it cycles during the water oxidation reaction; in the model of Kok,<sup>6</sup> these have been labeled as five S states (Scheme II).

Since the elucidation of the S-state cycle, the accessible states have been the objects of intensive study, both to gain information about the structure of the manganese cluster and to arrive at an understanding of the role of the cluster in the overall chemical and physical scheme of PSII. However, only  $S_1$  and  $S_2$  are readily accessible from the dark state of the enzyme, which, at physiologic pH and after short dark adaptations, is thought to contain a 3:1 mixture of  $S_1$  and  $S_0$ .<sup>6</sup> After long dark adaptations,  $S_1$  is exclusively formed.<sup>7,8</sup> The EPR-active  $S_2$  state has been formed by exposure of a dark-adapted PSII sample to single flashes at 273 K<sup>9</sup> or to continuous illumination while freezing<sup>10</sup> or at 195 K.<sup>11</sup> Herbicides

### Scheme I



### Scheme II



such as DCMU that bind to the  $Q_B$  site, and thereby restrict PSII to one stable charge separation, have also been used to great

(1) Brudvig, G. W.; Beck, W. F.; de Paula, J. C. *Annu. Rev. Biophys. Biophys. Chem.* 1989, 18, 25-46.

(2) (a) Dismukes, G. C.; Ferris, K.; Watnick, P. *Photobiochem. Photobiophys.* 1982, 3, 243-256. (b) de Paula, J. C.; Beck, W. F.; Brudvig, G. W. *J. Am. Chem. Soc.* 1986, 108, 4002-4009. (c) Kim, D. H.; Britt, R. D.; Klein, M. P.; Sauer, K. *J. Am. Chem. Soc.* 1990, 112, 9389-9391. (d) Bonvoisin, J.; Blondin, G.; Girerd, J.-J.; Zimmermann, J.-L. *Biophys. J.* 1992, 61, 1076-1086.

(3) Thompson, L. K.; Brudvig, G. W. *Biochemistry* 1988, 27, 6653-6658.

(4) Buser, C. A.; Thompson, L. K.; Diner, B. A.; Brudvig, G. W. *Biochemistry* 1990, 29, 8977-8985.

<sup>†</sup> Present address: Department of Chemistry, University of Connecticut, Storrs, CT 06269.